AgriEngineering

MDPI

Article

Predictive Modelling of *Amaranthus hybridus* Emergence Under Climate Change: Implications for the Efficiency of Bean and Maize Crop Systems

Emerson Cristi de Barros [1,2,*], Gefferson Pereira da Paixão [1], José Augusto Amorim Silva do Sacramento [3], Paulo Sérgio Taube [4,*] and João Thiago Rodrigues de Sousa [4]

[1] Department of Agricultural Engineering, Federal University of Viçosa, Viçosa 36570-900, MG, Brazil; gefferson.paixao@ufv.br
[2] Institute of Artificial and Computational Intelligence, Federal University of Viçosa, Viçosa 36570-900, MG, Brazil
[3] Multidisciplinary Centre of Barra, Federal University of Western Bahia, Barreiras 47100-000, BA, Brazil; jassacramento@yahoo.com.br
[4] Institute of Biodiversity and Forests, Federal University of Western Pará, Santarém 68035-110, PA, Brazil; thiagronomo@yahoo.com.br
* Correspondence: emerson.barros@ufv.br (E.C.d.B.); pstjunior@yahoo.com.br (P.S.T.)

Abstract

Climate change poses a significant challenge to food security, as it alters crop productivity, distribution patterns, and the overall food supply. This study modelled the emergence of *Amaranthus hybridus* L. in bean (*Phaseolus vulgaris* L.) and maize (*Zea mays* L.) production systems in the Brazilian state of Minas Gerais, in the cities of Coimbra, Paracatu, São João del-Rei, and Uberaba, under the Coupled Model Intercomparison Project Phase 6 (CMIP6) SSP1-2.6 and SSP5-8.5 scenarios. Using Hydrothermal Time (HTT), computational modelling, and nonlinear Weibull regression, weed emergence was simulated under current and future climate scenarios for 2050 and 2070. Although biological triggers such as temperature and base water potential remain constant, higher average temperatures accelerate HTT accumulation. Thus, this results in earlier and more intense emergence flows. The highest and lowest cumulative emergence were observed in Uberaba and Paracatu, respectively. The SSP5-8.5 scenario projects high emergence windows for 2070. This reduces the time available for management interventions. The root-mean-square error (RMSE) associated with the coefficient of determination (R^2) of the models validates HTT as an essential tool in computational agriculture. The integration of these models into decision-support systems is essential to mitigating productivity losses and it will increase control efficiency amid future climate uncertainties.

Keywords: computational agriculture; decision support systems; predictive modelling; hydrothermal time modelling; weed emergence dynamics; *Amaranthus hybridus*

Check for updates

Academic Editors: You Wu, Xianhua Wu, Zhibin Sun and Yufeng He

Received: 17 March 2026
Revised: 7 May 2026
Accepted: 8 May 2026
Published: 13 May 2026

Copyright: © 2026 by the authors. Licensee MDPI, Basel, Switzerland. This article is an open access article distributed under the terms and conditions of the Creative Commons Attribution (CC BY) license.

1. Introduction

Modern agriculture will face the challenge of increasing food production while adapting its crops to climate change. According to the Sixth Assessment Report (AR6) of the Intergovernmental Panel on Climate Change (IPCC), increasing global temperatures and altered precipitation regimes will affect crop production. It will interfere with the phenology and geographic distribution of weed communities [1]. In this context, weed emergence will determine the success of control strategies [2].

Among weeds with significant economic impact, the *Amaranthus* genus stands out for its high phenotypic plasticity, rapid growth, and high seed production [3]. Then, *Amaranthus hybridus* L. can aggressively compete for light, nutrients, and water [3]. The literature indicates that early-season weed interference from this genus can reduce crop productivity by more than 23% [4]. Furthermore, the economic damage threshold of 0.09–0.13 weeds per m^2 is very low, highlighting the severity of *Amaranthus* species on crops [3]. However, planning this management under climate change scenarios requires tools that transcend reliance on chronological time, since plant development is governed by biophysical variables [5].

Hydrothermal Time (HTT)-based modelling is an important approach for predicting seedling emergence [6,7]. The HTT concept integrates soil temperature and water potential (Psi) into a single cumulative metric, recognising that germination occurs only when both parameters exceed specific biological thresholds: the base temperature (Tb) and the base water potential (Psib) [6,7].

Fundamental studies have shown that, although the emergence calendar varies with annual fluctuations, the intrinsic biological response of seeds to the accumulation of thermal and water energy tends to be stable [2]. Therefore, the application of HTT in mathematical models, such as the Weibull equation, enables the development of predictive models with strong generalisation across different locations and future scenarios [8].

In the Brazilian state of Minas Gerais, the diversity of soils and microclimates requires a regioregionalized analysis. The mesoregions of Minas Gerais exhibit distinct water regimes, which directly influence weed establishment [9,10].

The use of high-resolution climate data from CMIP6 and Inmet, along with physical–hydraulic soil properties derived from global databases such as SoilGrids, enables precise spatialisation of pest risk. The integration of these technologies into computational agriculture enables the development of Decision Support Systems (DSS) that help producers optimise pesticide use and adjust planting windows to maximise competitiveness [11].

Despite the advances, there is still a gap in understanding how the different greenhouse gas emission scenarios, the Shared Socioeconomic Pathways (SSP), will affect synchronicity between crops and weed. The SSP1-2.6 scenario represents a sustainability trajectory, while the SSP5-8.5 scenario projects a severe worsening of thermal conditions [12,13].

Understanding whether global warming will lead to more concentrated or more distributed emergence flows is vital for the efficiency of production systems. If emergence accelerates, producers will face narrower operational windows, increasing pressure on application logistics and favouring the evolution of resistance if management is not diversified [14]. The central hypothesis is that future temperature increases will shorten the time required for the infestation to reach full establishment, necessitating a restructuring of management systems to maintain productive efficiency in the state.

The present study aimed to simulate the emergence of *A. hybridus* in four agricultural hub cities in the Brazilian state of Minas Gerais and to compare the Baseline period and the future projections for 2050 and 2070. The study sought to validate the robustness of the Weibull model based on HTT and to identify how variations in water balance and soil water potential act as environmental filters for the species.

2. Materials and Methods

All modelling, simulations, analyses and graphs were generated in the R v4.3+ environment [15].

2.1. Characterisation of the Study Areas and Target Species

The core objective of this research is to evaluate how the germination and emergence dynamics of *A. hybridus* are modulated by climate change until 2050 and 2070. Simulations were spatially allocated to four representative agricultural regions in the state of Minas Gerais, Brazil: Uberaba (19.85° S, 48.05° W; Triângulo Mineiro mesoregion), Paracatu (17.30° S, 46.80° W; Northwest mesoregion), São João del-Rei (21.13° S, 44.26° W; Campo das Vertentes mesoregion), and Coimbra (20.85° S, 42.80° W; Zona da Mata mesoregion) [16]. These locations represent important agricultural centres with distinct climatic conditions for the cultivation of *Phaseolus vulgaris* L. and *Zea mays* L. The species *A. hybridus* was selected for its relevance as a weed in these cropping systems and its high adaptability and ability to survive herbicide applications. To ensure a robust assessment of these biological responses, four locations in Minas Gerais (Brazil) were selected to represent distinct climatic envelopes and agricultural hubs.

The selection of these locations was based on their representativeness of the main producing mesoregions of Minas Gerais, encompassing the edaphoclimatic and socioeconomic diversity of the state. Tropical Savannas (Uberaba and Paracatu) represent the high-productivity (Mesoregions of Triângulo and Noroeste), characterised by large mechanised areas and water regimes that vary from typical tropical to seasonal (Aw, Köppen) [16–18]. Subtropical transition zones (São João del-Rei (Cwb, Köppen) and Coimbra (Cwa, Köppen)) represent transitional regions with higher humidity (Mesoregions of Campo das Vertentes and Zona da Mata) cultivated by small farmers, where the relief and climate favour distinct cultivation cycles [19–21]. This network of locations allows emergence models to be tested in different soil and climate scenarios for *P. vulgaris* and *Z. mays* crops in the state. The edaphic characterisation for the 0–5 cm layer was derived from the SoilGrids v2.0 database. These locations encompass a gradient of soil textures, which, combined with the aforementioned climatic diversity, allows for a systematic analysis of how environmental filters, specifically the interaction between temperature and water potential (Psi), influence the accumulation of Hydrothermal Time (HTT).

Amaranthus hybridus L., called amaranth or wild amaranth, is an annual herbaceous plant belonging to the Amaranthaceae family. It is notable for its vigorous growth and dense inflorescences. It has a high seed production and reported cases of herbicide resistance. According to Lorenzi (2014), its morphology exhibits great plasticity, adapting easily to different soil and climate conditions, which favours its wide geographic distribution in anthropised areas [22].

2.2. Obtaining Edaphoclimatic and Pedofunctional Data

The physical properties of the soil in the surface layer (0–5 cm) were extracted from the SoilGrids v2.0 database at a 250 m resolution [23]. The particle-size fraction data (sand, silt, and clay) were processed to estimate soil water parameters using pedofunctions [18]. Field capacity and permanent wilting point were calculated to determine the available water:

$$\theta_{PWP} = -0.024 * S + 0.487 * C + 0.006 + 0.005 * S - 0.013 * C + 0.068 * (S * C) + 0.031; \quad (1)$$

$$\theta_{FC} = \theta_{PWP} + 0.278 - 0.25 * S + 0.034 * C + 0.022 * (S * C) \quad (2)$$

where S is the sand fraction, and C is the clay fraction (g g^{-1}). The soil water potential (Ψ) as a function of volumetric moisture (θ) was estimated following the exponential relationship [24]:

$$\psi = -0.033 * exp \cdot \left(\frac{ln 1.5/0.033}{\theta_{FC} - \theta_{PWP}} \right) * (\theta_{FC} - \theta) \quad (3)$$

2.3. Climate Change Scenarios (CMIP6/MIROC6)

Baseline data were downloaded from Inmet for the period 2008 to 2024 (https://portal.inmet.gov.br/ (accessed on 9 October 2025)). For future projections, data from the MIROC6 global circulation model, obtained from WorldClim v2.1 (CMIP6) (www.worldclim.org (accessed on 9 October 2025)), were used. Two socioeconomic pathways (SSPs) were applied in two-time horizons: (1) SSP1-2.6: Optimistic scenario with low emissions (2050 and 2070) [12,13]; (2) SSP5-8.5: Pessimistic scenario with high emissions (2050 and 2070) [12,13].

The MIROC6 was established for climate prediction due to improvements in its representation of convection and cloud approaches. It results in more precise precipitation simulations in tropical and subtropical areas of Latin America than CMIP5 models [13–25]. Furthermore, MIROC6 exhibits balanced climate sensitivity, making it a reliable reference for agricultural impact studies that rely on the close interaction between temperature and soil moisture [25–27].

The Delta Change technique was applied to correct bias and spatialize the projections [28]. The monthly deltas for maximum temperature (Tmax), minimum temperature (Tmin), and precipitation rate (Prec) were extracted from the WorldClim v2.1 database (www.worldclim.org) and applied to the historical series:

$$T_{furure} = T_{hist} + \Delta T; \tag{4}$$

$$Preci_{future} = Preci_{hist} \cdot \left(\frac{Preci_{modelo_{fut}}}{Preci_{modelo_{hist}}} \right) \tag{5}$$

The climate simulated is shown in Figures 1 and 2.

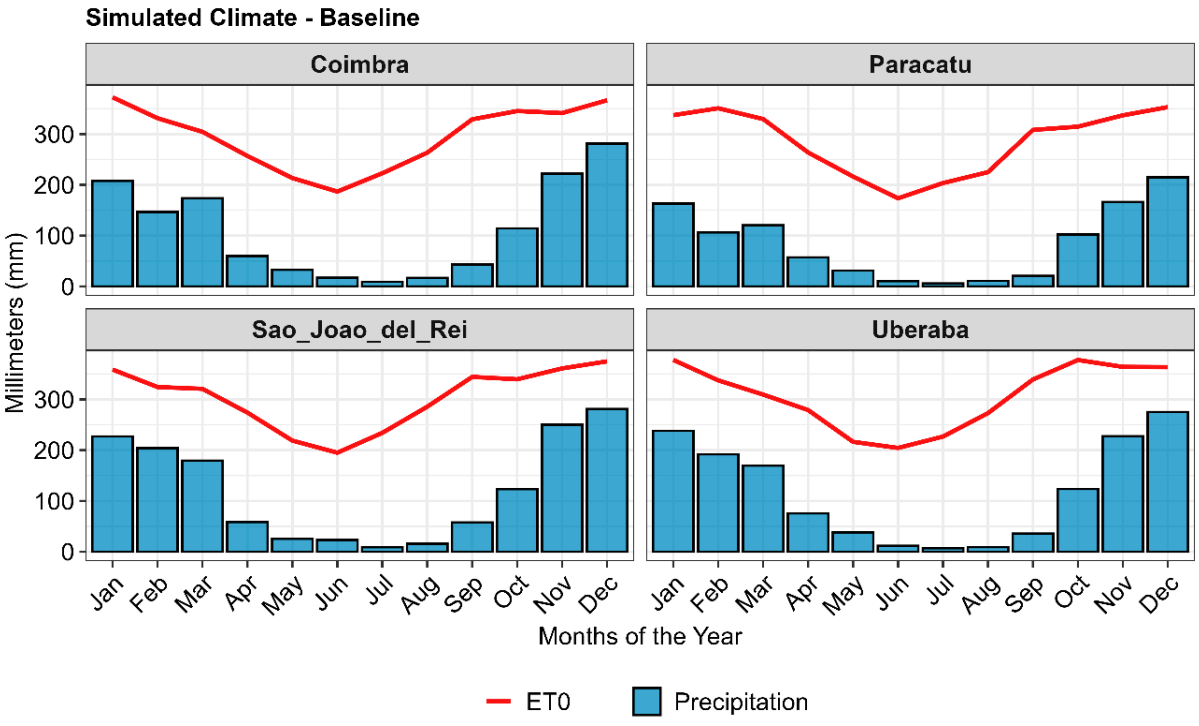

Figure 1. Simulated climate of Evapotranspiration (ETO) (mm) and Precipitation (mm).

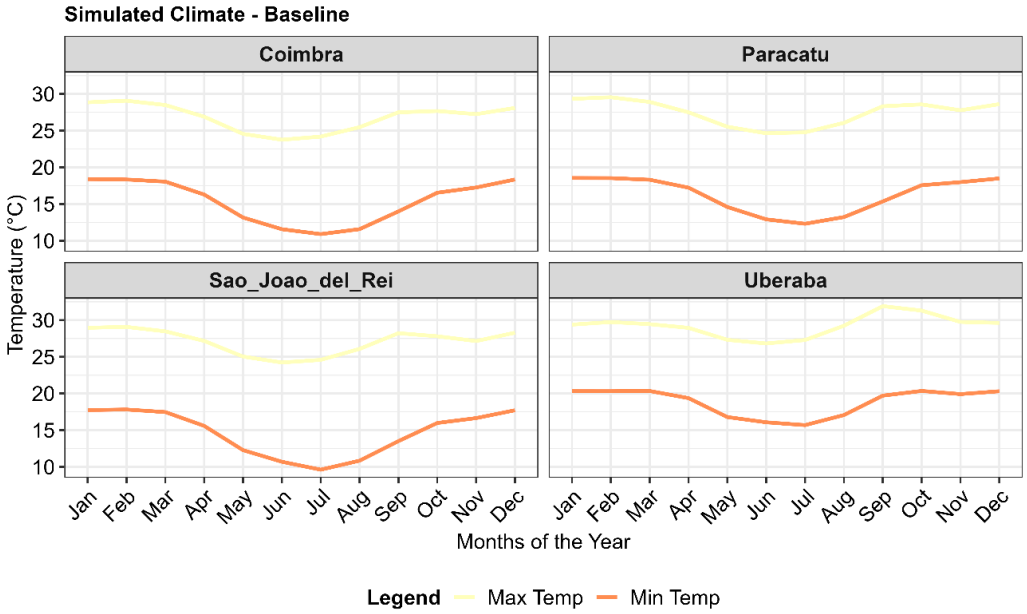

Figure 2. Simulated climate of Temperature minimal (°C) and Temperature maximum (°C).

2.4. Biophysical Modelling of Emergencies

We used the Hargreaves–Samani method to determine reference evapotranspiration (ETO. We used extraterrestrial radiation, based on latitude and the day of the year (J), to calibrate it [29].

$$ET_0 = -0.0023 * (T_{med} + 17.8) * \sqrt{(T_{max} - T_{min})} * R_a \quad (6)$$

The Penman–Monteith method is the FAO's gold standard, as noted in the literature. However, the Hargreaves–Samani method is the best choice for climate change simulations when future deltas (WorldClim) only give Tmax, Tmin, and precipitation. This is because it keeps the model simple without introducing bias from artificially generated wind or humidity in the future [11]. For us, WorldClim's future scenario includes no changes in radiation, humidity, or wind. The Hargreaves–Samani method is often better, or at least as good as, other methods because it was designed not to rely on these assumptions.

2.5. Hydrothermal Time (HTT)

The emergence of *A. hybridus* was modelled using the Accumulated HTT concept, which integrates temperature and water potential above baseline values [2,5]:

$$HTT = \sum max(0, T_{med} - T_b) * max(0, \psi_{soil} - \psi_b); \quad (7)$$

where the base temperature (Tb), obtained for *A. hybridus*, was defined as 9.6 °C and the base water potential (Ψ_b), for the *Amaranthus* genus, as −0.8 MPa [8,30]. The cumulative emergence percentage (E) was then described by a modified logistic/Weibull function [31]:

$$E = 100\left(1 - exp\left(\frac{HTT}{\alpha_w}\right)\right)^{\beta w}; \quad (8)$$

where α_w (85) is the scale parameter and (2,2) is the shape parameter. These parameters determine the slope of the emergence curve. These parameters were adopted based on literature calibrations for species of the *Amaranthus* genus, which exhibit rapid, staggered emergence under optimal temperature and humidity conditions [8].

2.6. Crop Emergence Dynamics and Critical Period for Interference Prevention (CPWC)

The planting date was optimised for each city using a kernel density estimate (KDE) based on the probability of accumulated rainfall exceeding 20 mm within a 3-day interval, mimicking the producer's technical decision. Crop emergence (corn and beans) was calculated via accumulated Degree-Days (DD) [32]:

$$GD = \sum(T_{med} - T_{b.cultura}) \quad (9)$$

Emergence occurred when GD $\geq$ the emergence GD (60 for corn, 50 for beans). We used a base temperature of 10 °C for corn and beans [33]. From emergence, the Critical Period for Interference Prevention (CPWC) was defined, and weed emergence was monitored during the critical windows for each crop. For corn, the CPWC was defined as the interval of 15–50 days after emergence (DAE). This period corresponds to the transition from the vegetative stage V2 to the onset of floral differentiation (V10–V12), a time of maximum sensitivity to competition for nitrogen and light [34].

The CPWC for beans varies widely in the literature; for the simulation, it was set to 10–35 days after emergence (DAE). Due to its shallower root system and short cycle, the crop requires earlier control, with applications concentrated during the vegetative growth phase until the beginning of pre-flowering (R5) [35].

2.7. Statistical Procedure and Simulation

To deal with climate uncertainty, a Block Bootstrapping algorithm was applied. Thirty simulation iterations were performed for each scenario at each location. In each iteration, a synthetic year of 120 days for corn and 95 days for beans was constructed by resampling 11-day blocks from the historical series. The resulting climate data from this procedure are presented in Figures 1 and 2.

The choice of 30 interactions is based on the Central Limit Theorem, which is widely accepted in the modeling literature as the minimum sample size necessary for the distribution of the sample mean to approximate a normal distribution and for the standard error estimates to become reliable, ensuring the statistical stability of the emergence curves without excessively increasing the computational cost [36,37].

For the construction of the synthetic year, the Moving Block Bootstrap technique with 11-day windows was used. This block length was selected to preserve the temporal dependence structure and autocorrelation of meteorological variables (precipitation and temperature), maintaining the physical integrity of extreme events and dry spells, which would be lost in a simple daily resampling. The process consisted of randomly selecting continuous blocks from the historical record. After that, it ensures that the relationship between soil water potential (Psi) and thermal sum (HTT) reflects real, physically plausible climatic conditions [38,39].

The results were analysed by analysis of variance (ANOVA), and the means were compared using Tukey's test (HSD) at a 5% significance level. The coding of the statistical groups followed an identification matrix (Scenario, Location, Time), allowing visualisation of the significance in the bar graphs and response curves.

To quantify the sensitivity of the emergence rate (y) as a function of the continuous environmental variables Hydrothermal Time (HTT), daily water balance, and soil water potential (Ψ), the relationship between the water balance (Precipitation—ETO) and the emergence rate was modelled using Weibull regression models and second-order polynomial regression models.

3. Results

3.1. The Simulation of Cumulative Weed Emergence

The results demonstrated substantial linkages among the timing of the crucial period, localities, and anticipated climate change scenarios (Figure 3). There was a statistically significant difference between the CPWC Start and CPWC End of the critical time in all situations and locations.

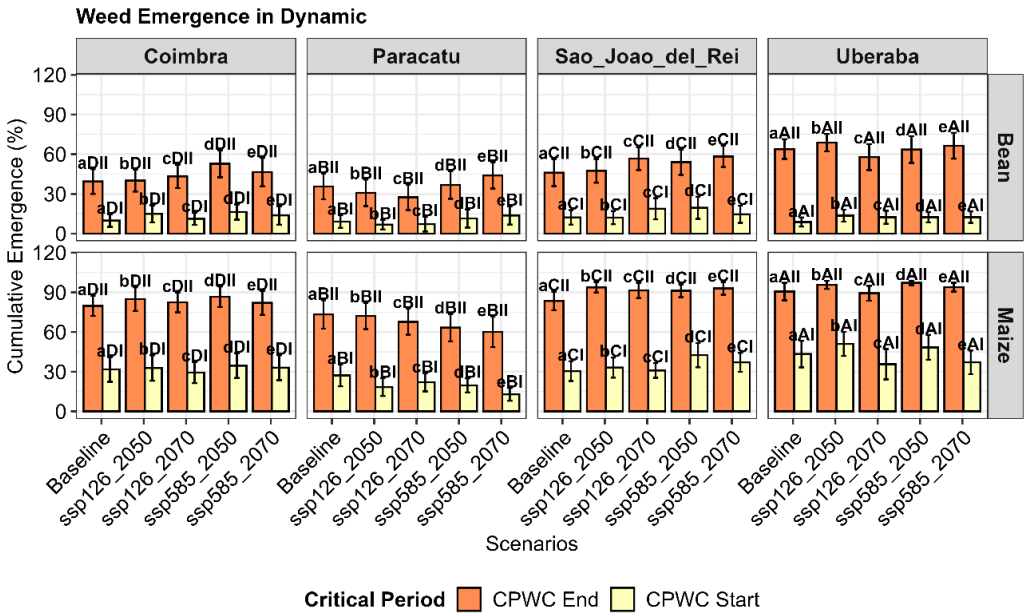

Figure 3. Cumulative weed seedling emergence (%) as a function of critical period and scenarios for bean and maize crops across four locations, Coimbra, Paracatu, São João del Rei, and Uberaba. Bars with different lowercase letters indicate differences between scenarios; bars with different uppercase letters indicate differences between cities; and bars with different Roman numerals indicate differences between critical periods.

The cumulative emergence at the end of the critical period (II) was always higher than at the beginning (I). This shows that new seedlings continued to arrive during the weed-interference interval, regardless of climate.

The cities emerged in different ways. Uberaba had the highest emergence rates. Then Coimbra and São João del-Rei acted as intermediaries. Paracatu also tends to have poorer emergence patterns. Climate change, however, affects emergence rates. In both cities (Bean and Maize), there was a distinct difference between the scenarios. This shows that both the time of year (2050 vs. 2070) and the severity of the emissions (SSP126 vs. SSP585) have a big effect on the proportion of plants that have grown (Figure 3).

The SSP585_2050 or SSP585_2070 scenarios usually have the highest averages. However, the Baseline (a) is usually the lowest average. It is recommended that a deteriorating climate may maintain or exacerbate weed pressure at the conclusion of the critical cycle in certain areas.

3.2. Cumulative Weed Seedling Emergence as a Function of Accumulated Hydrothermal Time

The non-linear Weibull model (Table 1, Figure 4) accurately captured the association between the total number of seedlings that emerged and the total amount of HTT to which weeds had been exposed in bean and maize crops. All of the places we looked at were Coimbra, Paracatu, São João del-Rei, and Uberaba. It showed that these models fit consistently (Table 1).

Table 1. Metrics and performance of the Weibull model for the accumulated hydrothermal time variable.

Crops	Cities	Scenarios	R^2	RMSE	b0	b1	b2
Bean	Coimbra	Baseline	1.00	0.13	96.60	1.78	88.60
Bean	Coimbra	SSP126_2050	1.00	0.18	126.60	1.67	111.88
Bean	Coimbra	SSP126_2070	1.00	0.16	96.17	1.76	87.63
Bean	Coimbra	SSP585_2050	1.00	0.43	93.88	1.81	85.44
Bean	Coimbra	SSP585_2070	1.00	0.31	106.47	1.59	99.29
Bean	Paracatu	Baseline	1.00	0.27	126.27	1.52	118.94
Bean	Paracatu	SSP126_2050	1.00	0.28	214.52	1.54	175.26
Bean	Paracatu	SSP126_2070	1.00	0.53	1549.43	1.32	1038.57
Bean	Paracatu	SSP585_2050	1.00	0.36	589.03	1.34	455.76
Bean	Paracatu	SSP585_2070	1.00	0.26	187.67	1.45	163.48
Bean	Sao_Joao_del_Rei	Baseline	1.00	0.22	87.33	1.88	80.98
Bean	Sao_Joao_del_Rei	SSP126_2050	1.00	0.25	106.49	1.84	95.19
Bean	Sao_Joao_del_Rei	SSP126_2070	1.00	0.15	100.58	1.93	89.67
Bean	Sao_Joao_del_Rei	SSP585_2050	1.00	0.65	93.53	1.82	84.61
Bean	Sao_Joao_del_Rei	SSP585_2070	1.00	0.38	92.18	1.96	84.26
Bean	Uberaba	Baseline	1.00	0.30	98.99	1.93	88.06
Bean	Uberaba	SSP126_2050	1.00	0.41	97.53	1.96	86.35
Bean	Uberaba	SSP126_2070	1.00	0.47	98.51	1.81	91.81
Bean	Uberaba	SSP585_2050	1.00	0.46	100.29	1.84	91.30
Bean	Uberaba	SSP585_2070	1.00	0.48	100.45	1.78	92.51
Maize	Coimbra	Baseline	1.00	0.49	100.38	1.74	92.40
Maize	Coimbra	SSP126_2050	1.00	0.54	98.13	1.71	89.93
Maize	Coimbra	SSP126_2070	1.00	0.71	101.10	1.75	94.64
Maize	Coimbra	SSP585_2050	1.00	0.61	99.80	1.66	92.85
Maize	Coimbra	SSP585_2070	1.00	1.04	98.44	1.64	92.39
Maize	Paracatu	Baseline	1.00	0.60	93.21	1.70	86.12
Maize	Paracatu	SSP126_2050	1.00	0.87	97.47	1.81	87.01
Maize	Paracatu	SSP126_2070	1.00	0.34	92.29	1.81	85.04
Maize	Paracatu	SSP585_2050	1.00	0.72	99.23	1.70	93.58
Maize	Paracatu	SSP585_2070	1.00	0.54	101.75	1.59	97.24
Maize	Sao_Joao_del_Rei	Baseline	1.00	0.47	99.48	1.78	91.42
Maize	Sao_Joao_del_Rei	SSP126_2050	1.00	0.62	98.82	1.90	87.64
Maize	Sao_Joao_del_Rei	SSP126_2070	1.00	0.90	99.35	1.89	88.36
Maize	Sao_Joao_del_Rei	SSP585_2050	1.00	0.53	99.51	1.83	90.23
Maize	Sao_Joao_del_Rei	SSP585_2070	1.00	0.72	99.08	1.85	88.65
Maize	Uberaba	Baseline	1.00	0.50	99.44	1.70	91.87
Maize	Uberaba	SSP126_2050	1.00	0.33	99.74	1.81	88.72
Maize	Uberaba	SSP126_2070	1.00	0.75	99.66	1.68	93.95
Maize	Uberaba	SSP585_2050	1.00	0.40	99.85	1.85	88.30
Maize	Uberaba	SSP585_2070	1.00	0.38	99.78	1.83	90.41

Note: Determination coefficient = R^2; Root mean square error (RMSE) and Slope coefficients = b0, b1 and b2.

This result shows that HTT is a strong predictor of initial development and that the Weibull equation effectively describes emergence kinetics in many situations. The curves fitted to the Baseline scenario and to the future projections (SSP126 and SSP585 for 2050 and 2070) had much in common. The emergence rate, when adjusted for the number of hydrothermal units in the Weibull model, stays the same. This means that plant biology will respond predictably to changes in temperature and water, even if the date of emergence changes in the future. So, it maintains each species' natural way of responding. After the first HTT concentration, weed growth in the common bean accelerated.

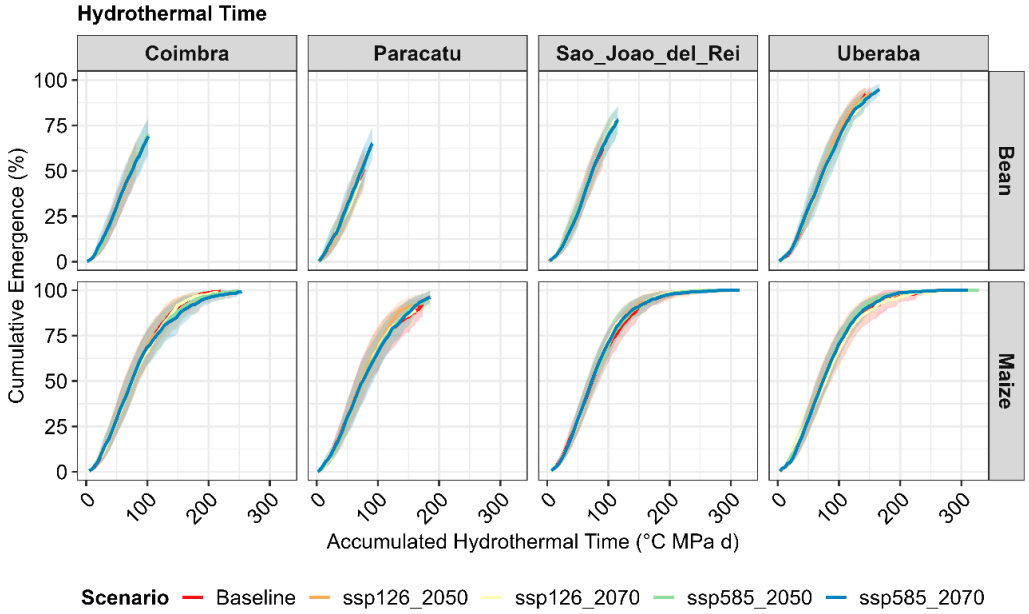

Figure 4. Cumulative weed seedling emergence (%) as a function of accumulated hydrothermal time (HTT, C MPa d) for weed of bean and maize crops across four locations, Coimbra, Paracatu, São João del Rei, and Uberaba. The panels illustrate the relationship under Baseline conditions and future climate change scenarios (SSP126 and SSP585 for the 2050 and 2070 periods). Solid lines represent the second-order polynomial regression models for each scenario, while the shaded areas indicate the 95% confidence intervals.

The model shows that 50% of emergence happens at about 100 °C MPa d. In Paracatu, the emergence changed more from one scenario to the next. Then, the shape of the Weibull curve stayed the same. The weed emergence trajectory was more uniform and comprehensive in corn. Most of the curves achieved the 100% emergence plateau between 200 and 250 °C MPa d. In this model, the upper asymptote (d) is the highest possible level of cumulative emergence.

The d parameter approached 100% in all maize cases. These facts show that something has fully and vigorously come into being. In the common bean, a greater variance in the asymptote was observed, with values stabilising between 75% and 90% across different locales. This fact implies that inherent or environmental variables constrained complete establishment under specific HTT settings.

The Slope Parameter (b) shows how fast anything comes out after the procedure starts. The high slope values observed in the curves for both crops indicate they emerge at the same time. Once the crucial HTT is reached, the shift from 0% to maximum emergence occurs quickly, which gives the curves their prominent sigmoidal form.

The inflexion or efficiency point (e) is the amount of HTT that must be added to reach approximately 63% of total emergence. This is commonly linked to T50 and in this case, the weed in the common bean needed less accumulation (around 100 °C MPa d) to achieve the same level of growth as the corn, which needed more (between 200 and 250 °C MPa d).

There was little difference across the climate change scenarios, and the Weibull model's high-quality fit indicates that phenological resilience is predictable. The growth rates of weed seedlings vary with temperature and moisture. This shows that the way crops grow tends to follow the same biological pattern across the four locations, regardless of weather conditions.

3.3. Emergence Rate as a Function of Daily Water Balance

Figure 5 and Table 2 show a positive, non-linear relationship between the amount of available water and the number of weeds.

Table 2. Metrics and performance of the quadratic polynomial model for the polynomial water balance variable.

Crops	Cities	Scenarios	R^2	RMSE	b0	b1	b2
Bean	Coimbra	Baseline	0.395	0.491	1.460	0.107	−0.008
Bean	Coimbra	SSP126_2050	0.401	0.490	1.411	0.125	−0.003
Bean	Coimbra	SSP126_2070	0.287	0.610	1.396	0.112	−0.004
Bean	Coimbra	SSP585_2050	0.321	0.663	1.707	0.148	−0.004
Bean	Coimbra	SSP585_2070	0.372	0.567	1.536	0.132	−0.003
Bean	Paracatu	Baseline	0.467	0.439	1.803	0.241	0.006
Bean	Paracatu	SSP126_2050	0.443	0.420	3.668	0.694	0.034
Bean	Paracatu	SSP126_2070	0.403	0.362	2.738	0.497	0.024
Bean	Paracatu	SSP585_2050	0.388	0.502	2.894	0.480	0.021
Bean	Paracatu	SSP585_2070	0.420	0.588	1.998	0.180	0.000
Bean	Sao_Joao_del_Rei	Baseline	0.335	0.535	1.463	0.110	−0.005
Bean	Sao_Joao_del_Rei	SSP126_2050	0.405	0.557	1.810	0.149	−0.005
Bean	Sao_Joao_del_Rei	SSP126_2070	0.386	0.606	1.857	0.111	−0.010
Bean	Sao_Joao_del_Rei	SSP585_2050	0.345	0.611	2.082	0.287	0.009
Bean	Sao_Joao_del_Rei	SSP585_2070	0.550	0.601	2.784	0.548	0.030
Bean	Uberaba	Baseline	0.465	0.787	2.153	0.188	−0.006
Bean	Uberaba	SSP126_2050	0.421	0.853	2.415	0.338	0.011
Bean	Uberaba	SSP126_2070	0.296	0.761	1.791	0.138	−0.003
Bean	Uberaba	SSP585_2050	0.268	0.818	2.010	0.173	−0.002
Bean	Uberaba	SSP585_2070	0.325	0.902	2.005	0.147	−0.005
Maize	Coimbra	Baseline	0.350	0.758	1.583	0.093	−0.005
Maize	Coimbra	SSP126_2050	0.274	0.883	1.498	0.085	−0.004
Maize	Coimbra	SSP126_2070	0.403	0.725	1.609	0.099	−0.004
Maize	Coimbra	SSP585_2050	0.346	0.890	1.580	0.088	−0.005
Maize	Coimbra	SSP585_2070	0.281	0.842	1.487	0.095	−0.002
Maize	Paracatu	Baseline	0.459	0.634	1.678	0.083	−0.006
Maize	Paracatu	SSP126_2050	0.483	0.665	1.835	0.110	−0.004
Maize	Paracatu	SSP126_2070	0.473	0.552	1.582	0.029	−0.008
Maize	Paracatu	SSP585_2050	0.482	0.523	1.659	0.028	−0.008
Maize	Paracatu	SSP585_2070	0.526	0.550	1.789	0.081	−0.004
Maize	Sao_Joao_del_Rei	Baseline	0.209	0.904	1.316	0.096	0.000
Maize	Sao_Joao_del_Rei	SSP126_2050	0.265	1.146	1.214	0.137	0.005
Maize	Sao_Joao_del_Rei	SSP126_2070	0.138	1.087	1.361	0.069	−0.004
Maize	Sao_Joao_del_Rei	SSP585_2050	0.238	1.022	1.409	0.130	0.002
Maize	Sao_Joao_del_Rei	SSP585_2070	0.224	1.089	1.458	0.094	−0.003
Maize	Uberaba	Baseline	0.345	0.926	1.319	0.174	0.008
Maize	Uberaba	SSP126_2050	0.312	1.063	1.554	0.202	0.006
Maize	Uberaba	SSP126_2070	0.209	0.875	1.436	0.105	−0.001
Maize	Uberaba	SSP585_2050	0.246	1.105	1.580	0.124	−0.004
Maize	Uberaba	SSP585_2070	0.312	0.993	1.570	0.180	0.005

Note: Determination coefficient = R^2; Root mean square error (RMSE) and Slope coefficients = b0, b1 and b2.

In all situations and locations, the emergence rate is close to zero or very low when the water balance is negative (i.e., values below 0 mm). This shows that water stress is the main factor preventing germination. The emergence rate increases rapidly as the balance becomes positive, indicating that rainfall exceeds evapotranspiration. Quadratic regression curves usually look like parabolas.

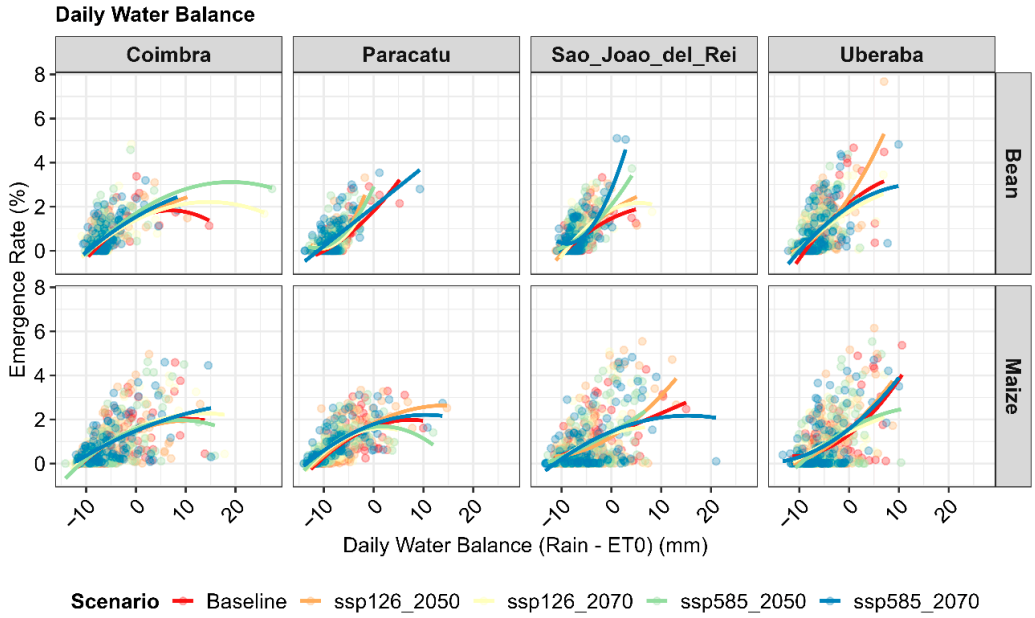

Figure 5. Emergence rate (%) as a function of Daily Water Balance (mm) for weeds of bean and maize crops across four locations, Coimbra, Paracatu, São João del Rei, and Uberaba. The panels illustrate the relationship under Baseline conditions and future climate change scenarios (SSP126 and SSP585 for the 2050 and 2070 periods). Solid lines represent the second-order polynomial regression models for each scenario, while the shaded areas indicate the 95% confidence intervals.

In certain cases, such as bean weeds in Coimbra, there is a plateau or a slight dip in very high water-balance values. This suggests that too much water may not cause emergence to rise steadily or may even saturate the system. Uberaba and São João del-Rei are two places where beans tend to sprout more quickly. This crop seems more sensitive to changes in water balance.

Emergence curves for maize are usually flatter, and the highest values are lower. This finding points to a more cautious response or a more spread-out emerging dynamic over time under the same water circumstances. There is a big difference in how cities and climate change scenarios (SSP126 and SSP585 for 2050 and 2070) respond to weed growth. The main difference across scenarios is seen in Uberaba. The SSP126_2050 scenario displays the highest weed emergence rate per millimetre of stored water in bean cultivation. This is much higher than the Baseline scenario. In the SSP585_2070 scenario, bean weeds in São João del-Rei respond aggressively.

The curve rises almost linearly and quickly reaches high rates after the water balance turns positive. The response amplitudes are lowest in Coimbra and Paracatu. The curves for all corn-weed scenarios in Paracatu are quite close to one another. This means that the emergence response to the water balance in this area should remain the same, regardless of future climate.

3.4. Emergence Rate as a Function of Soil Water Potencial

The following results about the emergence rate as a function of soil water potential are based on the analysis of Figure 6 and Table 3. The examination of the weed's biological response to soil water potential (Psi) revealed a non-linear relationship. The second-order polynomial models fit the best. The emergence rate has a positive, curvilinear relationship with the soil's potential to hold water. The emergence rate increases as the water potential approaches zero, indicating the soil becomes wetter.

Table 3. Metrics and performance of the quadratic polynomial model for the soil water potential variable.

Crops	Cities	Scenarios	R^2	RMSE	b0	b1	b2
Bean	Coimbra	Baseline	0.75	0.32	1.94	−2.00	−2.29
Bean	Coimbra	SSP126_2050	0.81	0.27	1.58	−2.96	−2.77
Bean	Coimbra	SSP126_2070	0.73	0.37	6.28	4.83	0.38
Bean	Coimbra	SSP585_2050	0.76	0.39	3.31	−0.90	−2.18
Bean	Coimbra	SSP585_2070	0.80	0.32	2.00	−2.93	−2.96
Bean	Paracatu	Baseline	0.82	0.26	6.76	5.61	0.69
Bean	Paracatu	SSP126_2050	0.79	0.26	8.69	8.03	1.45
Bean	Paracatu	SSP126_2070	0.82	0.20	−3.89	−10.67	−5.47
Bean	Paracatu	SSP585_2050	0.82	0.27	5.87	3.39	−0.41
Bean	Paracatu	SSP585_2070	0.83	0.32	3.48	−1.20	−2.42
Bean	Sao_Joao_del_Rei	Baseline	0.75	0.32	1.98	−1.92	−2.25
Bean	Sao_Joao_del_Rei	SSP126_2050	0.74	0.37	0.37	−5.22	−3.77
Bean	Sao_Joao_del_Rei	SSP126_2070	0.75	0.39	−0.27	−6.43	−4.29
Bean	Sao_Joao_del_Rei	SSP585_2050	0.69	0.42	1.07	−3.97	−3.24
Bean	Sao_Joao_del_Rei	SSP585_2070	0.69	0.50	6.61	4.25	−0.20
Bean	Uberaba	Baseline	0.79	0.50	13.42	15.45	4.26
Bean	Uberaba	SSP126_2050	0.78	0.53	11.25	11.91	2.87
Bean	Uberaba	SSP126_2070	0.74	0.46	5.96	2.97	−0.81
Bean	Uberaba	SSP585_2050	0.72	0.51	2.66	−2.67	−3.14
Bean	Uberaba	SSP585_2070	0.75	0.55	13.25	15.04	4.07
Maize	Coimbra	Baseline	0.38	0.74	1.98	−1.52	−2.09
Maize	Coimbra	SSP126_2050	0.40	0.81	4.93	3.76	0.18
Maize	Coimbra	SSP126_2070	0.48	0.68	7.37	7.35	1.52
Maize	Coimbra	SSP585_2050	0.44	0.83	7.04	7.35	1.68
Maize	Coimbra	SSP585_2070	0.32	0.82	−0.97	−7.31	−4.82
Maize	Paracatu	Baseline	0.63	0.53	5.96	4.54	0.25
Maize	Paracatu	SSP126_2050	0.64	0.55	8.85	8.91	1.90
Maize	Paracatu	SSP126_2070	0.63	0.46	−1.17	−7.42	−4.62
Maize	Paracatu	SSP585_2050	0.59	0.47	0.41	−5.07	−3.72
Maize	Paracatu	SSP585_2070	0.73	0.41	8.71	7.82	1.26
Maize	Sao_Joao_del_Rei	Baseline	0.29	0.85	5.45	5.63	1.28
Maize	Sao_Joao_del_Rei	SSP126_2050	0.37	1.06	10.72	16.44	6.49
Maize	Sao_Joao_del_Rei	SSP126_2070	0.23	1.03	8.88	12.53	4.59
Maize	Sao_Joao_del_Rei	SSP585_2050	0.25	1.01	2.33	−0.69	−1.80
Maize	Sao_Joao_del_Rei	SSP585_2070	0.22	1.09	4.74	4.29	0.65
Maize	Uberaba	Baseline	0.38	0.90	10.69	15.11	5.48
Maize	Uberaba	SSP126_2050	0.32	1.06	11.00	15.06	5.18
Maize	Uberaba	SSP126_2070	0.24	0.86	3.16	1.00	−0.91
Maize	Uberaba	SSP585_2050	0.26	1.10	8.20	10.04	2.98
Maize	Uberaba	SSP585_2070	0.29	1.01	14.15	19.86	7.05

Note: Determination coefficient = R^2; Root mean square error (RMSE) and Slope coefficients = b0, b1 and b2.

Weeds were quite sensitive to changes in water levels in the bean crop. In this situation, the maximum emergence rate is higher than that of maize in practically all places. In Uberaba, particularly in the SSP126_2050 scenario, the emergence rate neared 8%, the highest figure recorded in the study. Maize, on the other hand, had more subtle development curves and emergence rates that rarely went beyond 4%. This suggests that maize needs more heat and water to reach germination peaks than beans do under the same Psi circumstances.

The four cities that were looked at have different ways of spreading out and responding. In Uberaba, the highest emergence rates and steepest curves stood out. This means that the edaphoclimatic conditions were more conducive to rapid emergence when the humidity was right. In São João del-Rei, on the other hand, the raw data (points) were more spread out. The patterns in future scenarios, especially SSP585_2070, show that the emergence rate will increase at lower water potentials.

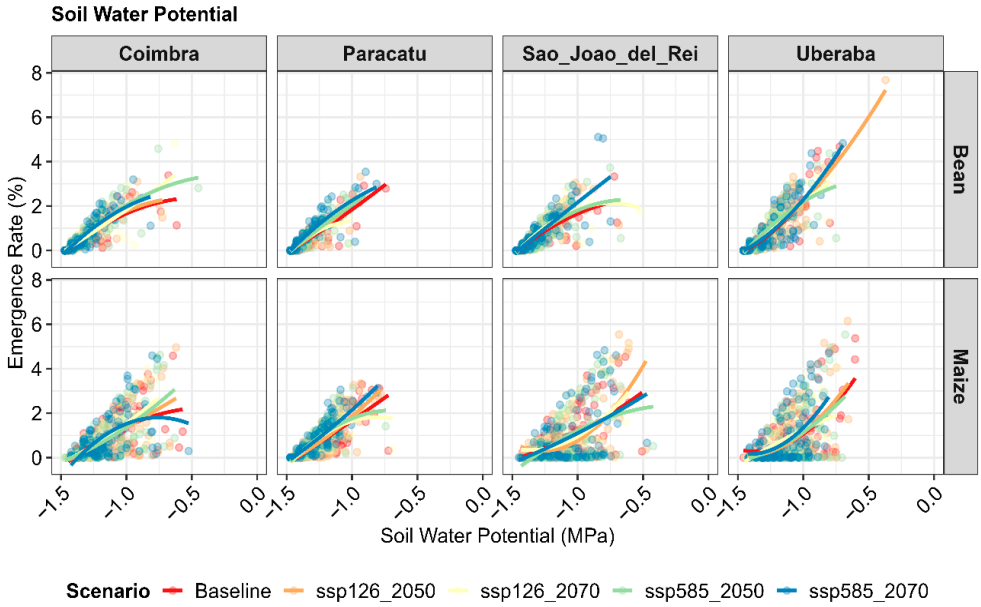

Figure 6. Emergence rate (%) as a function of Soil Water Potential (MPa) for weeds of bean and maize crops across four locations, Coimbra, Paracatu, São João del Rei, and Uberaba. The panels illustrate the relationship under Baseline conditions and future climate change scenarios (SSP126 and SSP585 for the 2050 and 2070 periods). Solid lines represent the second-order polynomial regression models for each scenario, while the shaded areas indicate the 95% confidence intervals.

The emergence curves in Coimbra and Paracatu reached a plateau between 2% and 4% and showed less variation across different climate scenarios. The curves changed because of future projection models (SSP126 and SSP585). In several cases, forecasts for 2050 and 2070 indicated higher emergence rates than the Baseline at the same Psi level. This suggests that a rise in average temperature may accelerate the emergence of metabolism, provided water is not the limiting factor.

The SSP585_2070 scenario often had a steadier linear slope, whereas the SSP126_2050 scenario tended to respond faster with less water.

3.5. The Validation Measures (RMSE and R^2)

The RMSE and R^2 indicate that the regression fit adequately explains changes in the emergence rate. This allows us to forecast how weeds and crops will behave under future water-stress conditions (Tables 1–3). The spread of the points (the coloured "dots") for Hydrothermal Time, water balance and water potential indicates that all these variables are a good predictor.

3.6. Otimal Planting Times

We used the probability density analysis (KDE) to identify the optimal planting times for beans and corn across the four sites we examined. These times were then added to the simulation. The best time to plant beans is around the beginning of March and maize around November.

Synchronous behaviours were seen at Coimbra (4 March), Paracatu (1 March), and São João del-Rei (3 March) (Figure 7). Uberaba, on the other hand, exhibited an earlier best date of 14 February. Its density curve was more spread out, giving it a more flexible planting window, although the weather was more variable throughout that time. There was a convergence in the corn crop at the end of November. The planting dates that were found were 16 November in Coimbra, 17 November in Paracatu, 15 November in São João

del-Rei, and 21 November in Uberaba. The results for scenarios versus the emergence of bean and maize are shown in Appendix A Figure A1.

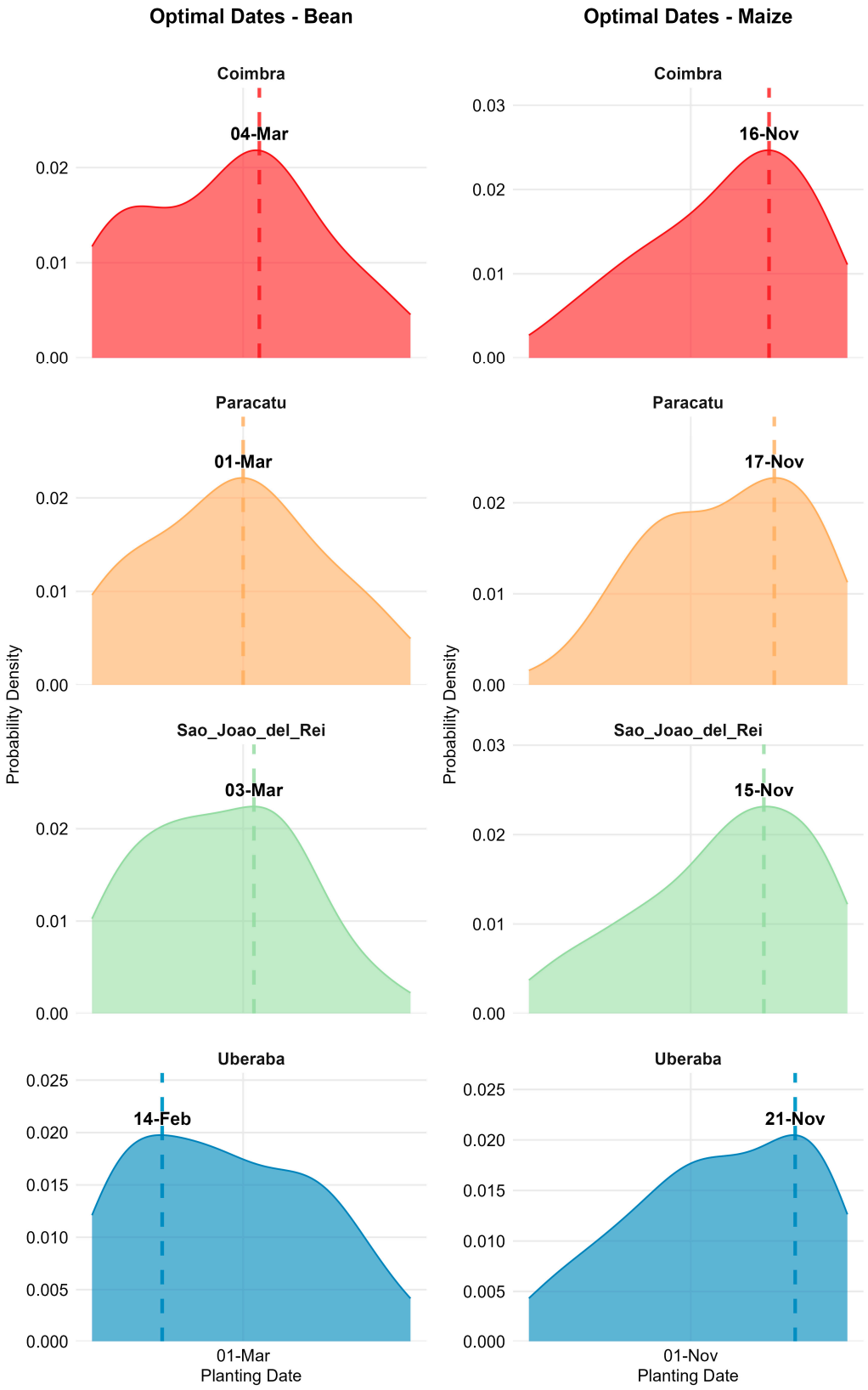

Figure 7. Kernel density of estimated optimal days to crop planting for bean and maize across four locations under the Baseline scenario. The line represents the optimal planting data, calculated based on the kernel density of probability.

4. Discussion

4.1. Regional Differences

The statistical disparities observed between the four cities in Brazilian state of Minas Gerais highlight the importance of spatially explicit modelling in biological systems. Uberaba presented the highest accumulated emergence rates, which can be attributed to the combination of soils with favourable water properties, estimated by pedofunctions, and thermal regimes that accelerate the accumulation of HTT [24].

Paracatu, on the other hand, has the most stable emergence patterns. Soil characteristics of this city shows that the area's poor water retention and balance make it hard to grow plants. The seed's biological clock stops when the soil water potential (Psis) approaches or falls below the baseline potential (Psib) of −0.8 MPa [40].

The differences between Uberaba and Paracatu can be ascribed to the HTT. In Uberaba, the water balance figures show that the soil water potential (Psi) remains predominantly above this threshold during the first 20 days after planting, resulting in a more linear and rapid HTT accumulation, reaching the scale parameter (αw) of 85 –day MPa in a shorter time interval.

On the other hand, in Paracatu, the analysis of environmental variables indicates greater stress. Although high temperatures favour the thermal component of the model, the frequent occurrence of dry spells causes Psi to decline sharply, reaching values below −1.0 MPa at various points during the critical imbibition phase. Since HTT accumulation is halted whenever Psi < Psib, the seed development 'clock' is repeatedly interrupted. This mechanism explains why, in Paracatu, emergence is not only slower but also presents a lower asymptote, as indicated by the high b0 and b2 values in Table 1, reflecting a seed population that remains in a state of dormancy induced by lack of water in the soil, even under ideal thermal conditions.

4.2. Impacts of Climate Change

Climate change will not affect all areas uniformly, as seen by regional sensitivity. The robust adjustment of the HTT across all climate scenarios (Baseline, SSP1-2.6, and SSP5-8.5) demonstrates that, although the civil calendar of emergence is altered by climate change, the biological triggers of the species remain preserved with respect to energy accumulation [2,5].

Water stress might reduce weed numbers due to physical constraints. At the same time, areas like the Uberaba will experience more aggressive infestations that occur earlier. The difference between the SSP1-2.6 and SSP5-8.5 scenarios was striking, especially in 2050 and 2070. The results showed that, in the extreme scenario SSP5-8.5, greenhouse gas emissions tend to increase the cumulative emergence at the end of the Critical Period for Interference Prevention (PCPI). This phenomenon is explained by the increase in average temperature, which acts as a metabolic catalyst.

4.3. Biological Stability of HTT Response

Unlike models that consider only temperature, such as Degree-Days, the HTT approach used here allowed us to identify that the thermal increase translates into greater emergence only when soil moisture is maintained. In 2070 scenarios, we observed that emergence windows become more "explosive": Thus, HTT accumulation occurs over a shorter time interval. These concentrated weed interferences shortly after the establishment of corn and bean crops. These facts reduce the window of opportunity for post-emergence interventions. Then, it requires more proactive management tactics.

A critical finding is the relationship between the parabolic patterns of emergence rate and water balance. Low or zero emergence in negative balances confirms that water deficit is the main environmental "filter" for *A. hybridus*. However, stabilisation or a slight drop at extremely high water balance values, as observed in Coimbra, suggests limitations due to anoxia or reduced soil temperature caused by excess moisture.

Convergence was observed, in which the accumulated emergence followed a consistent sigmoid pattern throughout the Weibull model. This fact corroborates the fundamental premise that a non-linear integration between temperature and water availability governs the initial development of weeds. The stability of the Weibull model parameters, especially the inflexion point (e) and the slope rate (b), suggests that *A. hybridus* exhibits functional homeostasis in its germination response. Our data indicate that the species requires a critical accumulation of hydrothermal units to initiate massive emergence flows, which constitutes a weed strategy to ensure establishment under conditions favourable to survival [41,42].

Modelling based on water potential (Psis) revealed that the common bean is more sensitive to moisture fluctuations than maize. Emergence rates in the common bean reached higher peaks at potentials close to zero. This fact suggests that the germination dynamics of *Amaranthus* are optimised to coincide with the moist soil conditions required by the common bean, making this crop particularly vulnerable to early competition.

4.4. Optimum Planting Data and PCPI

The KDE-generated planting windows revealed distinct operational challenges. For corn, the convergence to the second half of November places the PCPI in a period of high thermal and water availability, which favours the vigour of *A. hybridus*. As corn requires a longer PCPI, up to 50 DAE, the total accumulation of emergence (CPWC End) is drastically higher than at the beginning (CPWC Start), indicating that late flow control will be the biggest challenge for producers in Minas Gerais in the future.

For the common bean, although the cycle is shorter, the weed emergence speed (T50 close to 100 °C MPa d) requires that control be carried out at the beginning of the Critical Period of Prevented Interference, with a possible second application at the end of this period. The anticipated planting window in Uberaba, starting in February, suggests the crop may escape HTT peaks. However, it increases reliance on accurate climate forecasts to avoid severe water stress at the start of the cycle.

4.5. Limitations of the Model

Overall, these findings demonstrate that hydrothermal dynamics, rather than temperature alone, are key drivers of future weed emergence patterns, reinforcing the importance of integrating climatic and soil-water variables in predictive weed management models.

One inherent limitation of the present model, and one that should be central to future discussions, is the assumption that the baseline biological parameters (Tb and Psib) will remain constant until 2070. In reality, weeds, such as *Amaranthus* spp., are organisms endowed with exceptional phenotypic plasticity and the capacity for short-term adaptive evolution [20]. By fixing Tb at 10 °C and Psib at −0.8 MPa, we ignore the possibility of natural selection of biotypes that are more tolerant to heat or drought. If the species evolves to reduce its Psib, it can germinate in drier soils. Thus, the emergence projections for 2070 presented here would, in fact, underestimate reality. The rapid evolution of herbicide resistance in the *Amaranthus* genus has already demonstrated that this plant has a genome highly sensitive to selective pressures [43]. Therefore, the model should be interpreted as a "biological reference" scenario, over which adaptive evolution may overcome even greater infestation pressures.

The use of the Hargreaves–Samani method for calculating reference evapotranspiration (ET_0), although it differs from the Penman–Monteith standard, is justified by its scientific integrity in the absence of projected wind and solar radiation data in WorldClim v2.1. According to Droogers and Allen (2002) [11], in scenarios of future uncertainty, simplified models that depend only on temperature tend to be more robust and less prone to cascading errors. Then, it results from assumptions about unmodeled variables. This choice preserves the reliability of water-balance estimates, which are fundamental to calculating HTT.

Although MIROC6 provides a solid physical basis for projections, using a single GCM means that the model's climate sensitivity conditions the results [25,28,44–46]. Using a single scenario may not capture the full range of uncertainties in multi-model scenarios, which often exhibit divergences, especially in the magnitude and direction of regional precipitation changes. Therefore, the results presented here should be interpreted as probabilistic trends under the boundary conditions of MIROC6, emphasising that variability between different climate models is a known source of uncertainty in long-term climate change studies [46–49].

5. Conclusions

Climate change is expected to accelerate the emergence dynamics of *A. hybridus* in the agricultural systems of the Brazilian state of Minas Gerais by increasing hydrothermal accumulation and shortening the time to peak infestation.

The Hydrothermal Time (HTT) model proved effective for predicting spatial and temporal patterns of weed emergence under future climate scenarios.

Regions such as Uberaba and São João del-Rei may pose a higher risk of rapid weed establishment, potentially increasing early crop interference and reducing the window for effective weed control.

These findings highlight the importance of incorporating hydrothermal dynamics into predictive weed management strategies under changing climatic conditions. Future studies should incorporate evolutionary niche modelling to adjust the Tb and Psib parameters over time, integrating population genetics with biophysical modelling.

Author Contributions: E.C.d.B.: Conceptualisation, Software, Validation, Formal analysis, Resources, Writing (Original Draft), Writing (Review & Editing) and Visualisation. G.P.d.P.: Supervision, Project administration. J.A.A.S.d.S.: Writing—Review & Editing. P.S.T.: Writing—Review & Editing. J.T.R.d.S.: Writing—Review & Editing. All authors contributed to the study conception and design. All authors have read and agreed to the published version of the manuscript.

Funding: The authors are grateful for funding from the Coordination for the Improvement of Higher Education Personnel-Brazil (CAPES), grant code 001, the National Council for Scientific and Technological Development (CNPq), and the Foundation for Supporting Research in the state of Minas Gerais (FAPEMIG).

Data Availability Statement: All data used in this work were public source.

Conflicts of Interest: The authors declare no conflicts of interest.

Appendix A

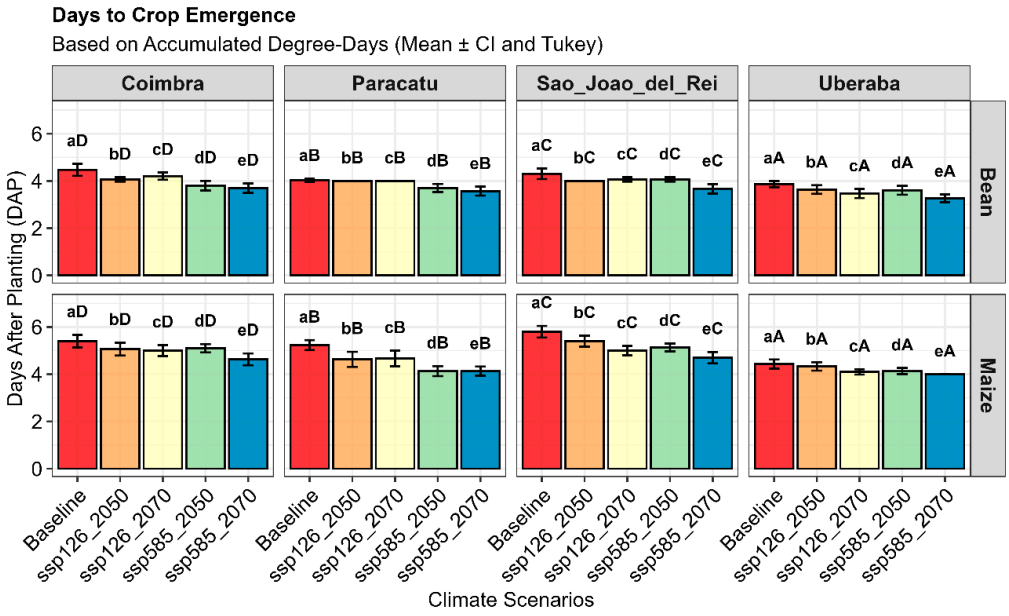

Figure A1. Crop emergency as a function of the current projection and the future. Bars with different lowercase letters indicate differences between scenarios and bars with different uppercase letters indicate differences between cities.

References

1. IPCC. Climate Change 2021: The Physical Science Basis. In *Contribution of Working Group I to the Sixth Assessment Report of the Intergovernmental Panel on Climate Change*; Masson-Delmotte, V., Zhai, P., Pirani, A., Connors, S.L., Péan, C., Berger, S., Caud, N., Chen, Y., Goldfarb, L., Gomis, M.I., et al., Eds.; Cambridge University Press: Cambridge, UK; New York, NY, USA, 2021.
2. Bradford, K.J. Applications of hydrothermal time to quantifying seed germination and emergence. *Weed Sci.* **2002**, *50*, 248–260. [CrossRef]
3. Vazin, F. The effects of pigweed redroot (*Amaranthus retroflexus*) weed competition and its economic thresholds in corn (*Zea mays*). *Planta Daninha* **2012**, *30*, 477–485. [CrossRef]
4. Inman, M.D.; Jordan, D.L.; Vann, M.C.; Hare, A.T.; York, A.C.; Cahoon, C.W. Influence of timing of Palmer amaranth control in dicamba-resistant cotton on yield and economic return. *Weed Technol.* **2020**, *34*, 682–688. [CrossRef]
5. Gummerson, R.J. The effect of constant temperatures and osmotic potentials on the germination of sugar beet. *J. Exp. Bot.* **1986**, *37*, 729–741. [CrossRef]
6. Meyer, S.E.; Debaene-Gill, S.B.; Allen, P.S. Using hydrothermal time concepts to model seed germination response to temperature, dormancy loss, and priming effects in Elymus elymoides. *Seed Sci. Res.* **2000**, *10*, 213–223. [CrossRef]
7. Watt, M.S.; Xu, V.; Bloomberg, M. Development of a hydrothermal time seed germination model which uses the Weibull distribution to describe base water potential. *Ecol. Modell.* **2010**, *221*, 1267–1272. [CrossRef]
8. Werle, R.; Sandell, L.D.; Buhler, D.D.; Hartzler, R.G.; Lindquist, J.L. Predicting Emergence of 23 Summer Annual Weed Species. *Weed Sci.* **2014**, *62*, 267–279. [CrossRef]
9. Coelho, G.L.N.; Carvalho, L.M.T.; Gomide, L.R. Modelagem preditiva de distribuição de espécies pioneiras no Estado de Minas Gerais. *Pesq. Agropec. Bras.* **2016**, *51*, 207–214. [CrossRef]
10. Sousa, E.P. Padrões Climáticos de Eventos Extremos de Chuva Utilizando Análise Multivariada e de Ondeletas no Estado de Minas Gerais. Doctoral Dissertation, Universidade Federal de Campina Grande, Campina Grande, Brasil, 2016.
11. Droogers, P.; Allen, R.G. Estimating reference evapotranspiration under inaccurate data conditions. *Irrig. Drain. Syst.* **2002**, *16*, 33–45. [CrossRef]
12. Hilal, K. Projected CMIP6 temperature changes over Sudan under SSP2-4.5 and SSP5-8.5 for mid- and late-21st century. *Met. Hydrol. Water Manag.* **2026**, *14*, 47–64. [CrossRef]
13. Kataoka, T.; Tatebe, H.; Koyama, H.; Mochizuki, T.; Ogochi, K.; Naoe, H.; Imada, Y.; Shiogama, H.; Kimoto, M.; Watanabe, M. Seasonal to decadal predictions with MIROC6: Description and basic evaluation. *J. Adv. Model. Earth Syst.* **2020**, *12*, e2019MS002035. [CrossRef]

14. Clements, D.R.; DiTommaso, A. Climate change and weed adaptation: Can evolution of invasive plants lead to greater range expansion than forecasted? *Weed Res.* **2011**, *51*, 227–240. [CrossRef]
15. R Core Team. *R: A Language and Environment for Statistical Computing*; R Foundation for Statistical Computing: Vienna, Austria, 2024. Available online: https://www.R-project.org/ (accessed on 1 October 2025).
16. Masukata, S.; Inoue, C.Y.A.; Sant'Anna, N.D.R.E. Global Environmental Governance and ODA from Japan to Brazil. In *Brazil—Japan Cooperation: From Complementarity to Shared Value*; Hamaguchi, N., Ramos, D., Eds.; Springer: Singapore, 2023. [CrossRef]
17. Alves de Melo, A.C.; Couto Júnior, A.F. O relevo como elemento organizador da ocupação antrópica na ecorregião do planalto central. *Espaç. Geogr.* **2022**, *21*, 154–177. [CrossRef]
18. Ofstehage, A.; Nehring, R. No-till agriculture and the deception of sustainability in Brazil. *Int. J. Agric. Sustain.* **2021**, *19*, 335–348. [CrossRef]
19. Neves, S.L.S.; Geraseev, L.C.; Augusto, H.A. Dos saberes tradicionais à agroecologia: Um estudo de caso das práticas agrícolas da comunidade vazanteira da Ilha do Jenipapo, Itacarambi-MG [Of traditional knowledge to agroecology: A case study of agricultural practices of the community vazanteira Island Jenipapo, Itacarambi-MG]. *Rev. Bras. Agroecol.* **2013**, *8*, 44–61.
20. Berg, L.; Roep, D.; Hebinck, P.; Teixeira, H.M. Reassembling nature and culture: Resourceful farming in Araponga, Brazil. *J. Rural. Stud.* **2018**, *61*, 314–322. [CrossRef]
21. de Carvalho Júnior, F.V.; de Carvalho Alves, M.; de Carvalho, L.G.; Pimentel, G.V.; Castilla Álvarez, C.E. Agroclimatic and Mechanization Zoning of Sugarcane Associated with Ethanol Production Potential in Minas Gerais Under Climate Change Scenarios. *J. Geovisualization Spat. Anal.* **2025**, *9*, 25. [CrossRef]
22. Lorenzi, H. *Manual de Identificação e Controle de Plantas Daninhas: Plantio Direto e Convencional*, 7th ed.; Instituto Plantarum: Nova Odessa, SP, Brazil, 2014.
23. Alvares, C.A.; Stape, J.L.; Sentelhas, P.C.; de Moraes Gonçalves, J.L.; Sparovek, G. Köppen's climate classification map for Brazil. *Meteorol. Z.* **2013**, *22*, 711–728. [CrossRef]
24. Poggio, L.; de Sousa, L.M.; Batjes, N.H.; Heuvelink, G.B.; Kempen, B.; Ribeiro, E.; Rossiter, D. SoilGrids 2.0: Producing soil information for the globe with quantified spatial uncertainty. *Soil* **2021**, *7*, 217–240. [CrossRef]
25. Saxton, K.E.; Rawls, W.J. Soil water characteristic estimates by texture and organic matter for hydrologic solutions. *Soil Sci. Soc. Am. J.* **2006**, *70*, 1569–1578. [CrossRef]
26. Tatebe, H.; Ogura, T.; Nitta, T.; Komuro, Y.; Ogochi, K.; Takemura, T.; Sudo, K.; Sekiguchi, M.; Abe, M.; Saito, F.; et al. Description and basic evaluation of simulated mean state, internal variability, and climate sensitivity in MIROC6. *Geosci. Model Dev.* **2019**, *12*, 2727–2765. [CrossRef]
27. Črnivec, N.; Cesana, G.; Pincus, R. Evaluating the Representation of Tropical Stratocumulus and Shallow Cumulus Clouds As Well As Their Radiative Effects in CMIP6 Models Using Satellite Observations. *J. Geophys. Res. Atmos.* **2023**, *128*, e2022JD038437. [CrossRef]
28. Hirota, N.; Michibata, T.; Shiogama, H.; Ogura, T.; Suzuki, K. Impacts of Precipitation Modeling on Cloud Feedback in MIROC6. *Geophys. Res. Lett.* **2022**, *49*, e2021GL096523. [CrossRef]
29. Navarro-Racines, C.; Tarapues, J.; Thornton, P.; Jarvis, A.; Ramirez-Villegas, J. High-resolution and bias-corrected projections of climate change for the agricultural sector. *Sci. Data* **2020**, *7*, 71. [CrossRef]
30. Hargreaves, G.H.; Samani, Z.A. Reference crop evapotranspiration from temperature. *Appl. Eng. Agric.* **1985**, *1*, 96–99. [CrossRef]
31. Loddo, D.; Ghaderi-Far, F.; Rastegar, Z.; Masin, R. Base temperatures for germination of selected weed species in Iran. *Plant Prot. Sci.* **2018**, *54*, 60–66. [CrossRef]
32. Grundy, A.C. Predicting weed emergence: A review of approaches and future challenges. *Weed Res.* **2003**, *43*, 1–11. [CrossRef]
33. McMaster, G.S.; Wilhelm, W.W. Growing degree-days: One equation, two interpretations. *Agric. For. Meteorol.* **1997**, *87*, 291–300. [CrossRef]
34. Renato, N.S.; Silva, J.B.L.; Sediyama, G.C.; Pereira, E.G. Influência dos métodos para cálculo de graus-dia em condições de aumento de temperatura para as culturas de milho e feijão. *Rev. Bras. Meteorol.* **2013**, *28*, 382–388. [CrossRef]
35. Kozlowski, L.A. Período crítico de interferência das plantas daninhas na cultura do milho baseado na fenologia da cultura. *Rev. Bras. Agrocienc.* **2002**, *8*, 121–125. [CrossRef]
36. Salgado, T.P.; Salles, M.S.; Martins, J.V.F.; Alves, P.L.C.A. Interferência das plantas daninhas no feijoeiro carioca. *Planta Daninha* **2007**, *25*, 443–448. [CrossRef]
37. Marchand, R.; Beagley, N.; Thompson, S.E.; Ackerman, T.P.; Schultz, D.M. A Bootstrap Technique for Testing the Relationship between Local-Scale Radar Observations of Cloud Occurrence and Large-Scale Atmospheric Fields. *J. Atmos. Sci.* **2006**, *63*, 2813–2830. [CrossRef]
38. Slaets, J.I.F.; Piepho, H.-P.; Schmitter, P.; Hilger, T.; Cadisch, G. Quantifying uncertainty on sediment loads using bootstrap confidence intervals. *Hydrol. Earth Syst. Sci.* **2017**, *21*, 571–588. [CrossRef]

39. Ebtehaj, M.; Moradkhani, H.; Gupta, H.V. Improving robustness of hydrologic parameter estimation by the use of moving block bootstrap resampling. *Water Resour. Res.* **2010**, *46*, W07515. [CrossRef]
40. Neves, R.T.; Costa, F.A. Unique Plant Adaptations to Varied Environments: A Comprehensive Review of Evolutionary Mechanisms Shaping Plant Survival Across Diverse Habitats. *Aust. Herb. Insight* **2020**, *3*, 1–5. [CrossRef]
41. Yettella, V.; Weiss, J.B.; Kay, J.E.; Pendergrass, A.G. An Ensemble Covariance Framework for Quantifying Forced Climate Variability and Its Time of Emergence. *J. Clim.* **2018**, *31*, 4117–4133. [CrossRef]
42. Frischie, S.; Fernández-Pascual, E.; Ramirez, C.G.; Toorop, P.E.; González, M.H.; Jiménez-Alfaro, B. Hydrothermal thresholds for seed germination in winter annual forbs from old-field Mediterranean landscapes. *Plant Biol.* **2019**, *21*, 449–457. [CrossRef] [PubMed]
43. Marcos Filho, J. *Fisiologia de Sementes de Plantas Cultivadas*; Abrates: Londrina, Brazil, 2015; p. 660.
44. Yanniccari, M.; Gaines, T.; Scursoni, J.; Prado, R.; Vila-Aiub, M. Global patterns of herbicide resistance evolution in *Amaranthus* spp.: An analysis comparing species, cropping regions and herbicides. *Adv. Weed Sci.* **2022**, *40*, e0202200037. [CrossRef]
45. Zubler, E.; Fischer, A.; Liniger, M.; Croci-Maspoli, M.; Scherrer, S.; Appenzeller, C. Localized climate change scenarios of mean temperature and precipitation over Switzerland. *Clim. Change* **2014**, *125*, 237–252. [CrossRef]
46. Paeth, H.; Steger, C.; Merkenschlager, C. Climate change—It's all about probability. *Erdkunde* **2013**, *67*, 203–222. [CrossRef]
47. Mamalakis, A.; Randerson, J.T.; Yu, J.-Y.; Pritchard, M.S.; Magnusdottir, G.; Smyth, P.; Levine, P.A.; Yu, S.; Foufoula-Georgiou, E. Zonally contrasting shifts of the tropical rain belt in response to climate change. *Nat. Clim. Change* **2021**, *11*, 143–151. [CrossRef] [PubMed]
48. Madsen, M.; Langen, P.; Boberg, F.; Christensen, J. Inflated Uncertainty in Multimodel-Based Regional Climate Projections. *Geophys. Res. Lett.* **2017**, *44*, 11606–11613. [CrossRef] [PubMed]
49. Shepherd, T. Atmospheric circulation as a source of uncertainty in climate change projections. *Nat. Geosci.* **2014**, *7*, 703–708. [CrossRef]

Disclaimer/Publisher's Note: The statements, opinions and data contained in all publications are solely those of the individual author(s) and contributor(s) and not of MDPI and/or the editor(s). MDPI and/or the editor(s) disclaim responsibility for any injury to people or property resulting from any ideas, methods, instructions or products referred to in the content.